Restoring the hydrologic response to pre-developed conditions in an urbanized headwater catchment: Reality or utopia?

Olivia Wright

A thesis submitted in partial fulfillment of the
requirements for the degree of

Master of Science

University of Washington
2013

Committee:
Erkan Istanbulluoglu
Jessica Lundquist

Program Authorized to Offer Degree:
Department of Civil and Environmental Engineering

University of Washington

Abstract

Restoring the hydrologic response to pre-developed conditions in an urbanized headwater catchment: Reality or utopia?

Olivia Wright

Chair of the Supervisory Committee:
Assistant Professor Erkan Istanbulluoglu
Department of Civil and Environmental Engineering

The conversion of forested areas to impervious surfaces, lawns and pastures alters the natural hydrology of an area by increasing the flashiness of stormwater generated runoff, resulting in increased streamflow peaks and volumes. Current stormwater infrastructure fails to offset the impact of increased impervious surfaces and loss of natural vegetation. The lack of adequate stormwater facilities along with increasing urbanization and population growth illustrates the importance of understanding urban watershed behavior and low impact development (LID) that focus on restoring the hydrology of an area. In this study, we developed a lumped urban ecohydrology model (UEM) that represents vegetation dynamics, connects pervious and impervious surfaces and implements various bioretention treatment scenarios. The model is applied to an urban headwater subcatchment located in the Newaukum Creek Basin. We evaluate the hydrologic impact of controlling runoff at the source and disconnecting impervious surfaces from the storm drain through model sensitivity analysis with varying sizes of bioretention cells. The model response to changes in storm depth, impervious area fraction, and treated area fraction of the urbanized catchment is assessed to identify the sensitivity of catchment variables in meeting hydrologic targets and goals. The effectiveness of the bioretention cells are quantified as the reduction in hydrologic indicators, high pulse count (HPC) and high pulse range (HPR), of the simulated basin

outflow as well as changes in the flow duration curves. Indicator results of model simulations show increasing bioretention cell size reached a ‘threshold of effectiveness’ for stream health improvement. In other words, after an initial improvement in indicator values associated with improved stream health, implementing larger bioretention cells to capture runoff from the same fraction of the basin did not significantly reduce indicators to further improve stream health. The bioretention cells were more effective at improving watershed conditions in drier climates or when total impervious fraction of the basin was reduced.

TABLE OF CONTENTS

LIST OF FIGURES

Figure Number *Page*

LIST OF TABLES

Table Number *Page*

ACKNOWEDGEMENTS

I am thankful for the guidance and encouragement provided by my advisor and committee chair Professor Erkan Istanbulluoglu during my Master's program. I am also thankful for the support of Jessica Lundquist and her help as a committee member. I am grateful for the time invested by Jim Simmonds, Rich Horner, Curtis DeGasperi, and Jeff Burkey in providing guidance throughout my study period.

1. INTRODUCTION

Urban development continues to replace forested areas with impervious surfaces, lawns and pastures, altering the natural hydrology of an area by increasing stormwater generated runoff and decreasing infiltration and recharge to groundwater. Without mitigation, the resulting stormwater runoff increases storm event peaks and volumes, with a greater potential to cause flooding and erosion. Stormwater runoff from urban areas transports more pollutants and nutrients to streams, impairing water quality. The cumulative effect of these changes alters in-stream habitat and impairs biologic health (May et al., 1997; PGCo, 1999b).

Studies conducted in the Puget Sound area of Washington have linked biologic health to flashiness and found stream health declined as urban development increased indicated by declining Benthic Index of Biological Integrity (B-IBI) scores associated with increasing total impervious area, (Fore, 1996; Horner et al., 1997; Morley and Karr, 2001; Booth et al., 2002; Booth et al., 2004; Fore et al., 2006;). B-IBI scores were highly variable at any given level of development revealing that degraded streams could occur at any level of development (Booth et al., 2004). Due to the ambiguity of impervious area revealing an accurate condition of stream health, studies have focused on identifying hydrologic metrics and indicators that provide a better link of biological response to urbanization (Booth et al., 2004; DeGasperi et al., 2009).

DeGasperi et al. (2009) identified hydrologic indicators that were most ecologically relevant for stormwater management in the Puget Sound lowlands. The study selected four criteria to select hydrologic indicators: (1) sensitive to urbanization, (2) demonstrates statistically significant trends in urbanized basins, (3) reflects the biological response to urbanization, and (4) insensitive to confounding variables (DeGasperi et al., 2009). Biological response was analyzed using observed B-IBI scores collected from King County, WA streams. The two indicators that best met the four criteria were High Pulse Count (HPC) and High Pulse Range (HPR) (DeGasperi et al., 2009; Horner, 2012). HPC is the number of times each water year that discrete high pulses occur. A high pulse is identified as a discrete exceedance above a threshold, or

twice the long-term mean flow rate. HPR is the range of days between first and last high pulse flow in water year.

B-IBI scores from the DeGasperi et al. (2009) data show a clear negative trend with increasing HPC and HPR values (Figure 1-1). Furthermore, there is a range of indicator values associated with different levels of biological health (Horner, 2012). The red lines in Figure 1-1(a) and (b) denote a transition in the observed data where indicator values become exclusively correlated with low B-IBI scores and poor stream health. The analysis resulted in the following hydrologic indicator ranges associated with various stream conditions (Table 1-1).

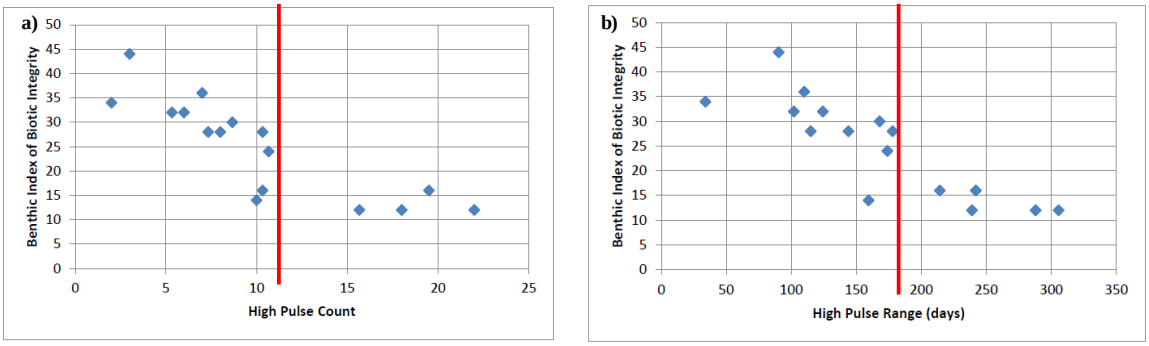

Figure 1.1. **B-IBI in relation to HPC (a) and HPR (b)** (Horner, 2012).

Table 1-1: **Hydrologic Indicator Target Ranges.**

B-IBI Goal	Stream Condition	HPC	HPR
> 35	Good	3.0 – 7.0	90 – 110
30 – 35	Fair	2.0 – 8.7	34 – 168
24 – 29	Poor	7.3 – 10.7	115 – 178
< 16	Very Poor	10.0 – 22.0	160 – 306

Stormwater management traditionally has focused on removing stormwater runoff from urban areas as quickly as possible to prevent flooding (i.e., grey stormwater management). This has been achieved by connecting impervious surfaces directly to curbs, gutters and pipe conveyance system for direct routing to streams or large, centralized stormwater facilities, such as a retention or detention pond (PGCo, 1999b; EPA, 2000; Davis, 2005). These approaches limit stormwater management to mitigating

impacts from a larger concentration of stormwater downstream of a drainage area. Furthermore, these structural measures have not been able to restore the natural hydrologic regime of the watershed in which local biota are adapted (May et al., 1997; Booth et al., 2002).

In the 1990's, Prince George's County, Maryland introduced a new technique in stormwater management emphasizing controlling runoff at the source with low impact development (LID) (Coffman, 2000; USEPA, 2000). LIDs mimic the natural hydrologic functions of the landscape with stormwater storage, infiltration, evaporation or detention techniques. LIDs reduce the impervious area directly connected to the storm drain and increase runoff travel time to reduce large accumulation of stormwater runoff volumes (PGCo, 1999, 1999b; USEPA, 2000). Development options include, but are not limited to, bioretention facilities, rain barrels, vegetative swales, vegetated rooftops, and porous pavements. LID can be applied to most areas of a catchment independent of the land use or the stage of development, whether it's new development, redevelopment or retrofits to existing development. This type of treatment is less intrusive than conventional stormwater management options since they can be placed in smaller available pervious space adjacent to impervious areas (Coffman, 2000; USEPA, 2000; Davis, 2005).

Despite the growing interest in green stormwater management, numerical models to evaluate the efficiency of green infrastructure are limited. Existing models usually treat green infrastructure facilities separate from the hydrological processes of the catchment and do not include vegetation dynamics. In this paper, we first develop the Urban Ecohydrology Model (UEM), a lumped ecohydrology model designed to evaluate the role of green stormwater management facilities integrated with the hydrologic processes in a catchment. The dynamic vegetation component in the model allows for the examination of different vegetation options and their influence on green infrastructure performance, which would be critical in water-limited regions as well as seasons. In this paper we focus on the use of UEM to evaluate the performance of bioretention facilities distributed across a small urban catchment located in the Puget Sound lowlands of Washington State. The effectiveness of the bioretention facilities are measured by their reduction in hydrologic indicators values, HPC and HPR, of the basin.

2. STUDY AREA AND DATA

The Puget Sound lowlands are located west of the Cascade Mountains in a maritime climate. The region has a maritime climate with dry summers and wet winters. Land use ranges from forested, agricultural, low to high density residential, and industrial (Herrera, 2007). Prior to development, the area was covered with coniferous forests.

Our catchment of interest is Newaukum Urban, a subcatchment of the Newaukum Creek Basin (Figure 2-1). Newaukum Creek is a southern tributary of the Green-Duwamish Watershed that flows from the mountains east of Enumclaw into the middle Green River. The mean annual precipitation of the basin is approximately 1246 mm/yr. Newaukum Urban is a relatively flat, highly developed subcatchment located in the city of Enumclaw. It is approximately 1 km^2 with 93.5% of the area urbanized (King County 2007 landuse cover) and 70% total impervious area (TIA) (King County 2009 Impervious Coverage). The basin's mean annual precipitation is 1246 mm. Soils are primarily sandy loam to loam (Latterell et al., 2007).

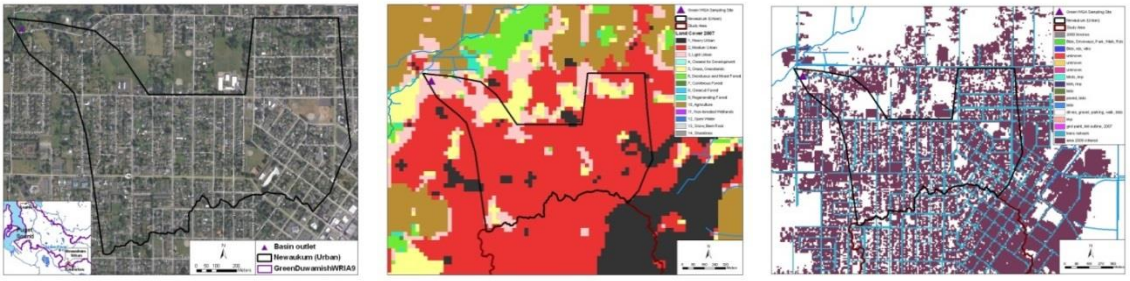

Figure 2-1**. Left: Newaukum Urban Google Maps, Center: King County 2007 landuse cover, Right: KingCounty 2009 Impervious Coverage.**

A study by Cuo et al. (2009) looked at five lowland Puget Sound basins that ranging from low (24%) to highly urbanized (71%). The mean annual runoff ratios (R/P) ranged from 0.33 to 0.61. Burges et al. (1998) studies a suburban and an undeveloped basin with runoff ratios 0.49 and 0.24, respectively. Although Newaukum Urban is more urbanized than any of the basins mentioned above, it has a runoff ratio of 0.23, which is much lower than the urbanized basin and more like the forested catchment in the Burges

et al. (1998) study. Table 2-1 presents the area of the impervious land use categories and the fraction of the basin they cover. Rooftop area was estimated from King County building footprint data (http://www5.kingcounty.gov/gisdataportal/Default.aspx). The 'other' category represents driveways, parking lots and other miscellaneous impervious surfaces in the catchment.

Table 2-1. **Impervious land cover area and fraction of basin.**

Impervious Category	**Area (acres)**	Fraction of Basin
Roads	41.32	0.15
Rooftop	24.92	0.09
Other	120.10	0.45
Total Impervious Area	**186.34**	**0.70**

Three years of observed hourly streamflow data is available for Newaukum Urban from 03/22/2001 to 10/13/2004 (Herrera, 2007; King County, 2002). Hourly precipitation and air temperature data were obtained from King County's Enumclaw rain gage (44u gage). The rain gage is approximately 4.2 km away from the outlet of Newaukum Urban and is 830 feet in elevation. All of King County's collected data can be downloaded at their Hydrological Info Center (http://green.kingcounty.gov/wlr/waterres/hydrology/). Incoming solar radiation data was gathered from Washington State University Puyallup AgWeatherNet location (http://weather.wsu.edu/awn.php). The station is approximately 24 km from the outlet of Newaukum Urban and 34 feet in elevation.

3. METHODS

3.1. Model Description

This study develops the lumped Urban Ecohydrology Model (UEM) to simulate the urban landscape and examine the impact of bioretention stormwater treatment at the catchment scale. The UEM lumps the catchment into pervious and impervious surface layers. The impervious surface layer is further partitioned into the effective impervious area (EIA) that is directly connected to the storm drain and the disconnected impervious area (DIA) that routes stormwater runoff to the pervious surface layer (Figure 3-1).

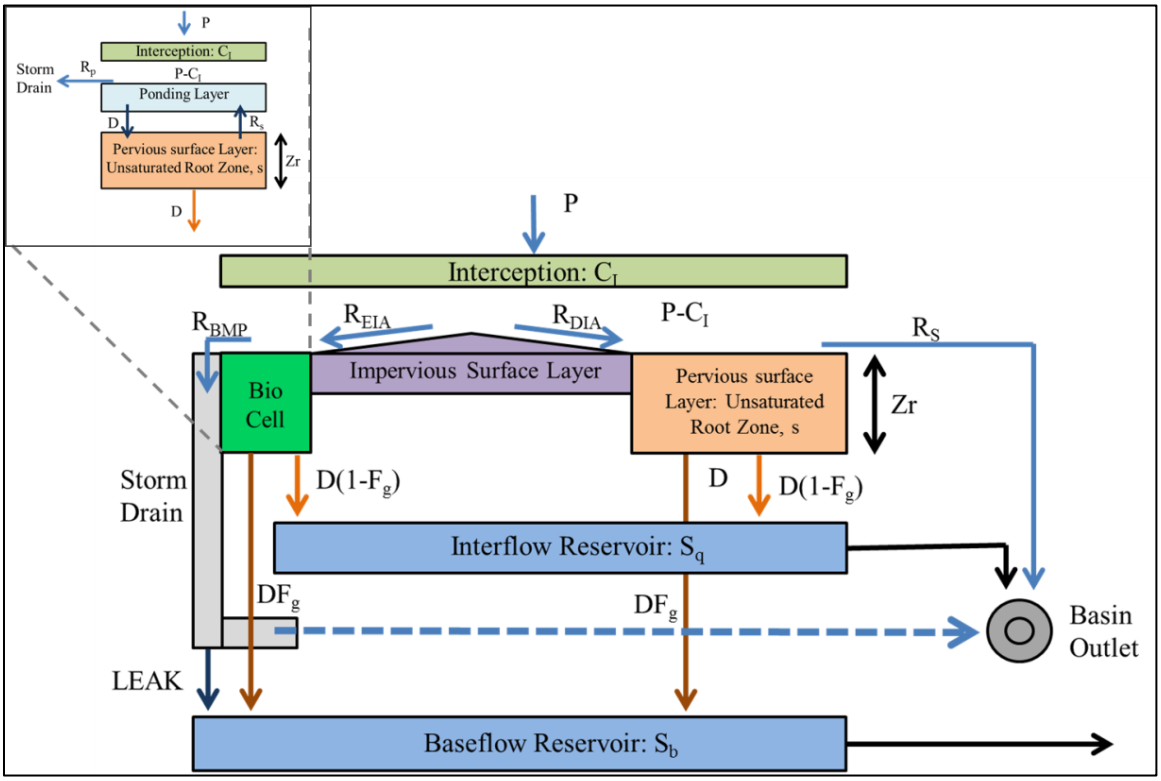

Figure 3-1**. Conceptual representation of the processes in the UEM.**

UEM integrates bioretention facilities (rain gardens) as part of the hydrologic system. Bioretention facilities are LIDs that use vegetation, soils, and additional storage to improve water quality and hydrology of an urbanized location (PGCo, 2007). Our bioretention cell conceptualization effectively represents individual bioretention cells distributed throughout the catchment. A bioretention cell is conceptualized as a pervious surface layer with amended soils and an additional ponding layer above the pervious soil layer. The bioretention cell captures stormwater runoff from the EIA before it reaches the storm drain, allowing for additional infiltration and storage in the catchment. Any accumulated runoff that exceeds the ponding depth is directly connected to the storm drain and discharged to a receiving water body. A single bioretention cell is assumed to have fixed dimensions that receive surface runoff from 1,000 ft^2 of effective impervious area. This design drainage area is estimated through an adaptive practice but may change as research develops in this area. The number of the bioretention cells across the

catchment are calculated by dividing the total area treated in the catchment by the design drainage area for each bioretention cell. The model divides the catchment to pervious and impervious area. Bioretention cells are assumed to be located within pervious areas.

In the model, the depth averaged soil moisture in the pervious surface root zone layer is calculated by the mass balance equation (Istanbulluoglu et al., 2012):

$$nZ_r \frac{ds}{dt} = [f(s,p,V) - ET(s,V) - D(s)] \quad (1)$$

where n [-] is the porosity, Z_r [L] is the effective rooting depth, s is soil moisture, t [t] is time, f [L/T] is the infiltration rate, ET_a [L/T] is the actual evapotranspiration rate, and D [L/T] is drainage. Interception from the canopy C_I [L/T] is calculated by:

$$C_I = \min(I_{max}V_{t,}PV_t) \quad (2)$$

where I_{max} [L] is the maximum hourly interception, V_t [-] is the fraction of vegetation cover on the land surface (includes dry and live biomass), and P [L] is depth of rainfall. When P is larger than C_I, throughfall occurs at the same rate as precipitation. The precipitation duration reaching the ground is reduced to account for initial filling of the canopy storage during the early part of the rain event.

The pervious input rate, p [L/T] is calculated as the depth of rainfall minus the canopy interception of the pervious surface layer and the precipitation depth minus the initial abstraction of the disconnected impervious fraction of the basin:

$$p = (P - C_I) + \frac{(P-I_a)\cdot(IMPfrac-EIAfrac)}{1-IMPfrac-BIOfrac} \quad (3)$$

where I_a [L/T] is the initial abstraction of the impervious surfaces, *IMPfrac* [-] is the basin impervious surface fraction, *EIAfrac* [-] is the basin effective impervious fraction that is directly connected to the storm drain, and *BIOfrac* [-] is the fraction of bioretention cells in the basin.

Basin saturation is calculated before and after a storm:

$$A_{sf1} = 1 - (1 - \frac{s}{1+b})^b \quad (4)$$

$$A_{sf2} = 1 - (1 - \frac{s+(P-I_a)/nZ_r}{1+b})^b \quad (5)$$

where s is soil moisture ($s = \theta/n$) before the storm, θ is the soil moisture volumetric water content, and b is the infiltration shaper parameter (Liang et al., 1994).

Total watershed infiltration before and after the storm is obtained from the Variable Infiltration Capacity (VIC) curve as a function of maximum watershed potential infiltration, Imax [L].

$$I_{max} = (1-b)nZr \quad (6)$$

$$I_1 = I_{max}[1 - (1 - A_{sf1})^{1/b} \quad (7)$$

$$I_2 = I_{max}[1 - (1 - A_{sf2})^{1/b} \quad (8)$$

Using the geometry of the VIC curve, surface runoff is estimated as:

$$R_s = (I_2 - I_1)(A_{sf1} - A_{sf2})/2 \quad (9)$$

The root zone layer is assumed to have uniform soil texture, porosity, and hydraulic conductivity. The drainage of the soil column by gravity is modeled to occur at the lowest boundary of the soil layer. At soil saturation, the drainage is at its maximum and is calculated as the saturated hydraulic conductivity (K_s) and decays exponentially to a value of zero at field capacity, s_{fc}. The drainage of the catchment with bioretention treatment includes additional drainage from the bioretention soil layer.

$$D(s) = \begin{cases} K_s(1 - IMPfrac - BIOfrac) + D_{bio}(BIOfrac), & s = 1 \\ K_s s^{2b+3}(1 - IMPfrac - BIOfrac) + D_{bio}(BIOfrac), & s_{fc} < s \leq s \end{cases} \quad (10)$$

where *K(s)* [L/T] is unsaturated hydraulic conductivity, *b* [-] is an empirical parameter in the Campbell soil moisture retention model (Campbell, 1974), and D_{bio} [L/T] is the drainage from the bioretention cell.

Catchment interflow and baseflow are calculated from a linear reservoir model. The rate of interflow R_q [L/T] is proportional to the interflow reservoir storage S_q [L].

$$R_q = (\frac{1}{T_q} S_q)(1 - IMPfrac) \quad (11)$$

where S_q is the interflow reservoir storage and T_q [T] is the interflow reservoir drainage time scales. Change in the reservoir storage is:

$$\frac{dS_q}{dt} = D\left(1 - F_g\right) - R_q \quad (12)$$

where D is drainage from the root zone [L/T], F_g is the fraction of drainage that goes to the groundwater reservoir. The rate of baseflow R_b [L/T] is proportional to the baseflow reservoir storage S_b [L].

$$R_b = (\frac{1}{T_b} S_b)(1 - IMPfrac) \quad (13)$$

where S_b is the baseflow reservoir storage and T_b [T] is the baseflow reservoir drainage time scales. Change in the reservoir storage is:

$$\frac{dS_b}{dt} = DF_g - R_b \quad (14)$$

Impervious surface runoff generated from the EIA and DIA must be identified to determine the fraction flowing to the storm drain and pervious surface respectively. Runoff from the disconnected impervious areas, R_{DIA} [L/T], is calculated as:

$$R_{DIA} = (P - I_a)(IMPfrac - EIAfrac) \quad (15)$$

Runoff from effective impervious areas, R_{EIA} [L/T], is calculated as:

$$R_{EIA} = (P - I_a) \cdot EIAfrac \cdot (1 - LEAK) \quad (16)$$

where *LEAK* [-] is the fraction of the EIA runoff lost from the stormwater sewer system. Total streamflow from the basin with no bioretention treatment, R [L/T], is calculated as:

$$R = R_s + R_b + R_{EIA} \tag{17}$$

Total streamflow from the basin with bioretention treatment is calculated as:

$$R = R_s + R_b + R_{BIO} \tag{18}$$

where R_{bio} [L/T] is the overflow from the bioretention ponding layer.

Actual evapotranspiration is calculated using a soil moisture limitation approach (Laio et al., 2001; Istanbulluoglu et al., 2011):

$$ET_a = PET \cdot \beta_s(s) \tag{19}$$

where *PET* is the potential evapotranspiration and β_s is an evapotranspiration efficiency term based on soil moisture, calculated as:

$$\beta_s(s) = \begin{cases} s & s_h < s < s_w \\ \frac{s - s_w}{s^* - s_w} & s_w < s < s^* \\ 1 & s^* < s \end{cases} \tag{20}$$

where s_h is soil hygroscopic capacity, s_w is soil moisture at wilting point, s^* is soil moisture at stomata closure (Laio et al., 2001). In equation (19), evaporation is at its potential rate when $s>s^*$, decaying linearly in response to soil moisture deficit when $s<s^*$ until the wilting point is reached (Laio et al., 2011a). When the surface is devoid of vegetation, s_w is replaced by the hygroscopic water content, s_h. A soil moisture retention curve (Campbell, 1974) can be used to calculate the threshold soil moisture values of s_{fc}, s^*, s_w, and s_h for different soil textures based on the corresponding soil matric potentials defined for soil and plant conditions (Pockman and Sperry, 1997, 2000):

$$s(\psi) = \left(\frac{\psi}{\psi_{ae}}\right)^b \tag{21}$$

where ψ [L] is the corresponding matric potential for s_{fc}, s^*, s_w, and s_h and ψ_{ae} [L] is air entry pressure.

Hourly potential evapotranspiration is calculated using the Priestly Taylor method:

$$PET = \alpha \frac{\Delta}{\Delta+\gamma} \left(\frac{R_N - G}{\rho_w \lambda_v}\right) \quad (22)$$

where Δ is the slope of the saturation vapor pressure – temperature relationship (kPa $^oC^{-1}$), R_N is net radiation at the evaporating surface (W/m^2), G is the ground heat flux (W/m^2), $\lambda_v \rho_w$ is the latent heat of vaporization (28.34 Wd m^{-2} mm^{-1}) or (680.16 Wh m^{-2} mm^{-1} for hourly), γ is the psychronometric constant (kPa $^oC^{-1}$), and α is an empirical constant (1.26 for humid climates).

3.1.1. Simulating Bioretention Facilities

Bioretention cells are modeled as a pervious area with amended soils for increased infiltration capacity and a ponding layer for additional storage. The depth averaged soil moisture in the pervious surface root zone layer of the bioretention cell is calculated by the mass balance equation:

$$nZ_r \frac{ds}{dt} = [f_{BIO}(s,p,V) - ET_{BIO}(s,V) - D_{BIO}(s)] \quad (23)$$

The ponding storage, *Pond* [L] is calculated as:

$$\frac{dPond}{dt} = \max(0, Inflow - D_{soil} - R_{BIO}) \quad (24)$$

where *Inflow* [L/T] is the incoming impervious surface runoff and precipitation and R_{BIO} [L/T] is the overflow of the ponding storage, producing bioretention cell runoff that is connected to the storm drain. D_{soil} [L/T] is the drainage from the ponding storage into the bioretention cell soil, calculated as:

$$D_{BIO}(s) = \begin{cases} K_s + f_{pond}) \cdot BIOfrac & s = 1 \\ K_s s^{2b+3} \cdot BIOfrac & s_{fc} < s \leq 1 \end{cases} \quad (25)$$

When the soil is unsaturated, the infiltration rate of the bioretention soil layer is estimated as the minimum of the precipitation rate and the infiltration capacity. After soil saturation, the infiltration rate is reduced to the drainage rate:

$$f_{BIO} = \begin{cases} \min[p, I_c] & 0 \le s < 1 \quad P > C_I \\ D, & s = 1, \quad P > C_I \end{cases} \tag{26}$$

where I_c is infiltration capacity and p is the average pervious input rate. Pooling, P_{depth} [L/T], begins to occur when the effective precipitation, (p=P-C_I), exceeds the infiltration capacity:

$$P_{depth} = \begin{cases} (p - I_c) & p > I_c \\ 0 & p \le I_c \end{cases} \tag{27}$$

The infiltration rate, f_{pond} [L/T], from the ponded storage into the bioretention cell soil is calculated as:

$$f_{pond} = \min(D_{soil}, Pond) \tag{28}$$

The runoff from the ponding layer of the bioretention cell is calculated as:

$$R_{BIO} = \begin{cases} 0 & Pond \le Pond_{max} \\ Inflow - \frac{dPond_{max}}{dt} & Pond > Pond_{max} \end{cases} \tag{29}$$

where $Pond_{max}$ [L] is the weir height of the ponding layer.

Evapotranspiration of the bioretention cell is calculated using the same method as the UEM pervious surface layer with equation (19).

3.1.2. Biomass Production

Vegetation dynamics are simulated on the pervious surface layer and bioretention soil layer. Hourly net primary productivity (NPP, g DM m^{-2} hr^{-1}) is allocated to surface and root biomass pools. NPP is calculated as (Istanbulluoglu et al., 2012):

$$NPP = 0.75(1 - \mu) \cdot ET_a \cdot WUE \cdot \rho_v \cdot w \tag{30}$$

where μ is the ration of nighttime to daytime CO_2 exchange, ET_a is actual evapotranspiration, WUE is the water use efficiency, p_v (kg m^{-3}) is water density, and *w* converst CO_2 gained to dry matter (kg DM kg^{-1} CO_2). We used the vegetation and soil parameters from Istanbulluoglu et al. (2012) BGM model.

3.2. Baseflow Separation

Estimating surface water runoff identifies the volume of water that can potentially be captured by BMPs to meet flow targets. The volume of surface water is estimated by subtracting calculated baseflow from the observed hydrograph using a recursive digital filter method for baseflow separation (*Nathan and McMahon*, 1990; *Chapman*, 1991). This technique establishes low frequencies of baseflow by removing high frequency signals of quickflow. Baseflow is calculated as:

$$Q_b(i) = kQ_b(i-1) + \frac{1-k}{2}[Q(i) + Q(i-1)] \quad (31)$$

where Q_b is the estimated baseflow [mm/hour], Q is measured daily streamflow [mm/hour], k is a filter parameter, recession constant, and i is the daily time step. The recession constant (k) is calculated by examining the receding limb of the hydrograph. The following equation is used to describe the recession curve (*Hino and Hasebe*, 1984; *Linsley et al.*, 1958):

$$Q_t(i) = Q_0 e^{-\alpha t} = Q_0 e^{-t/T_c} \quad (32)$$

where Q_t is discharge at time t, Q_0 is the initial discharge, α is a constant and T_c is the recession period. The reciprocal of T_c is equal to α and is also referred to as the cut off frequency (f_c). The term $e^{-\alpha}$ can be replaced by the recession constant k (*Hino and Hasebe*, 1984). Therefore:

$$k = e^{-\alpha} = e^{-f_c} \quad (33)$$

f_c is determined by plotting the natural log of the recession discharge ratio values ($\ln(Q_0/Q)$) on a semi-logarithmic axis (*Hino and Hasebe*, 1984; *Sujono et al.*, 2004).

Three different types of storage can contribute to streamflow: surface flow, subsurface flow and baseflow. These contributions result in a curved line on the semi-logarithmic plot and can be approximated by three straight lines along the recession curve (*Linsley et al.*, 1958). The slope of the last portion of the recession limb estimates the value of f_c. Results of the recursive digital filter method from two Newaukum Urban storm events are plotted in Figures 3-2 (a-f).

Our values of ln(Q_0/Q) plot as a curved line, implying that different types of storage contribute to streamflow. A baseflow index (BFI: baseflow-to-streamflow ratio) can be used to estimate baseflow contribution to streamflow. With baseflow estimated in equation (1), the long term BFI is calculated by (*Smakhtin*, 2001; *Wang et al.*, 2009):

$$BFI = \frac{\sum_{i=1}^{n} Q_b}{\sum_{i=1}^{n} Q} \tag{34}$$

where *n* is number of hourly time steps. Using all available hourly streamflow data for the basin, the calculated BFI for Newaukum Urban is 0.49.

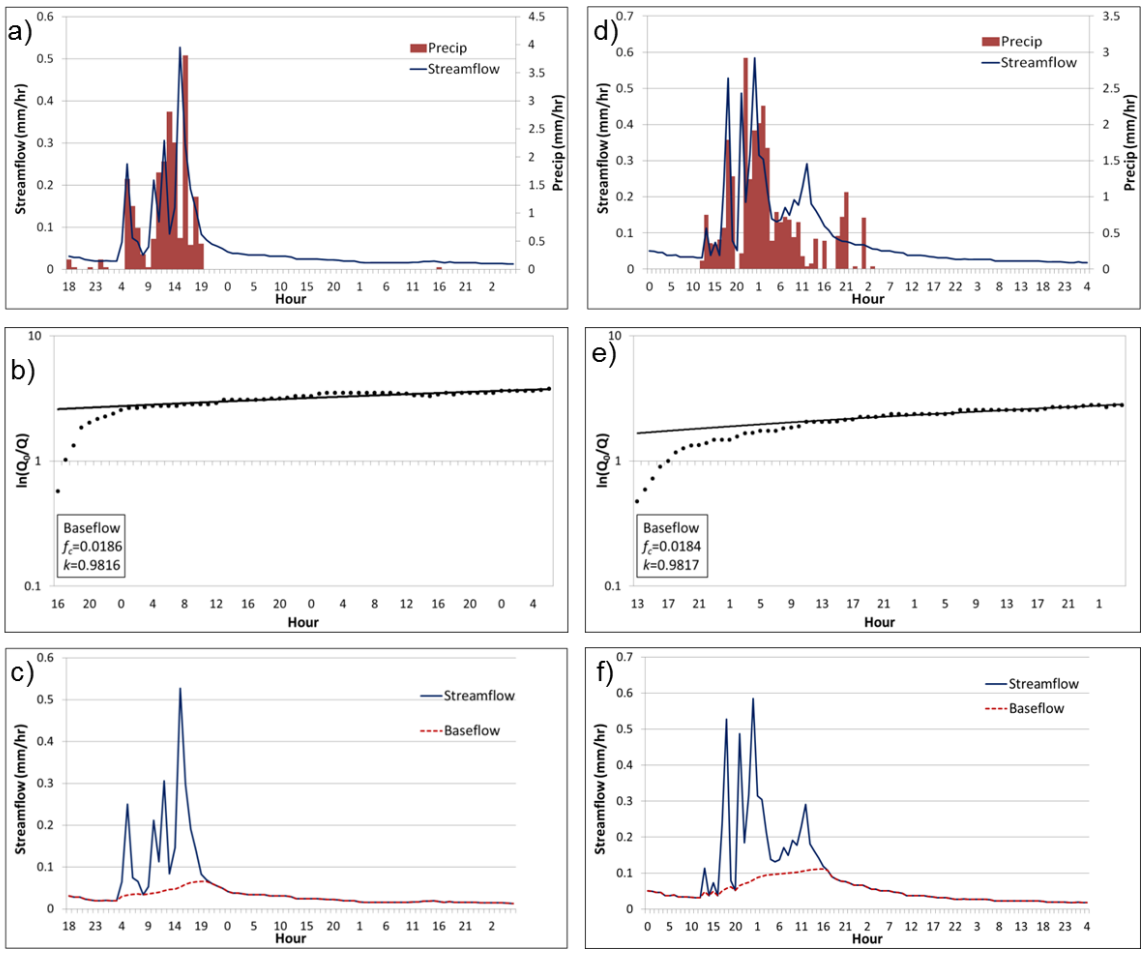

Figure 3-2**. (a-c) Newaukum Creek from 01.04.03 at 02:00 to 01.07.03 at 14:00, (d-f) Newaukum Creek from 04.01.01 at07:00 to 04.05.01 at 12:00. (a,c) Observed storm event and discharge, (b,e) plot of hydrograph recession limb to estimate recession constant, (c,f) baseflow separation.**

3.3. Rainfall-Runoff Depth Analysis

A rainfall-runoff depth analysis of storm events is used to estimate the effective contributing area of the basin and the initial abstraction of impervious surfaces (*Boyd et al.* 1993, 1994). The analysis evaluates the surface runoff depth estimated from baseflow separation of each storm as a function of the storm's precipitation depth. The slope of the relationship estimates the fraction of the basin that contributes to runoff and the rainfall axis intercept estimates the initial abstraction that must be satisfied before runoff can occur.

Storm events were calculated by summing consecutively occurring hourly precipitation. Individual storm events were separated by 24 hours of no precipitation. Due to the responsiveness of our basin, we assumed the runoff event occurred during the same time period as the precipitation event.

Our study focuses on dry season (fall/summer) storm events and assumes the basin contributes runoff from effective impervious areas only minus any loss from the stormwater sewer system during drier periods. Results from the rainfall-runoff depth plots with the initial abstraction removed are shown in Figure 3-3. Plotting all surface runoff storm events estimates an initial abstraction as 4 mm. Rainfall- surface runoff depth plots estimated approximately 15% of the basin contributes to runoff during the dry months. From the rainfall-runoff plot, surface runoff can be calculated as:

$$R = (P - I_a) \cdot EIA \cdot (1 - LEAK) \tag{35}$$

where P [L/T] is the storm depth, I_a [L/T] is the initial abstraction, *EIA* [-] is the effective impervious area fraction, and *LEAK* [-] is the fraction of stormwater runoff entering the sewer system. For input into the UEM, we estimate the *EIA* as 20% of the basin and *LEAK* as 25% of the stormwater runoff entering the sewer system, giving an average of 15% of the basin contributing to streamflow at each time step.

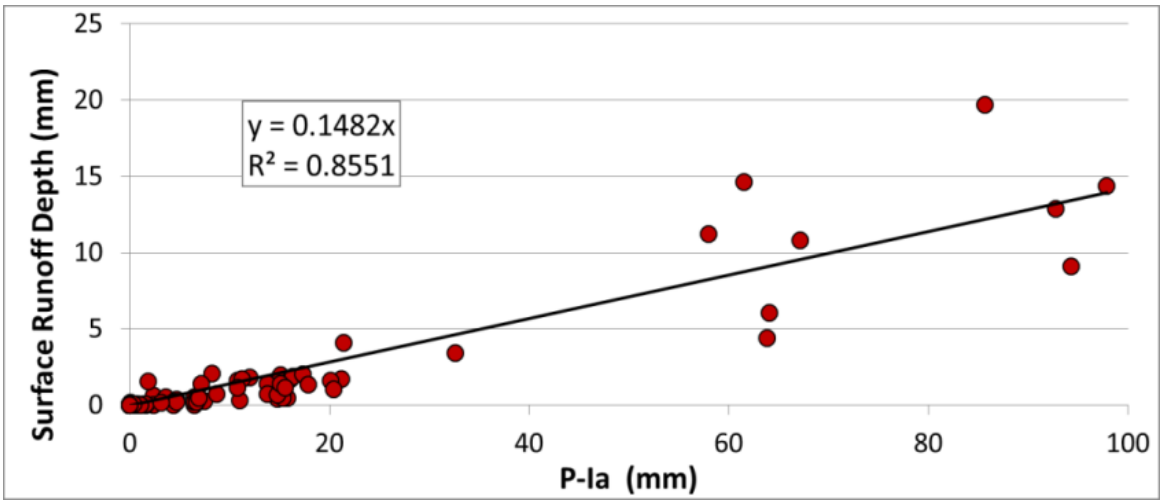

Figure 3-3**. Dry season (summer/fall) Rainfall-Runoff Analysis.**

4. RESULTS AND DISCUSSION

4.1. Model Calibration

The model with no bioretention treatment was calibrated to 3 years of hourly observed streamflow data. Three model parameters are used for calibration: *Fg* controls the fraction of drainage from the soil layer directly contributing to groundwater and subsurface flow, *T* controls the reservoir drainage timescale, and the Variable Infiltration Capacity (VIC) b-shape parameter controls the shape of the infiltration capacity curve. Model calibration was performed using flow duration curves and the Nash-Sutcliffe (NS) model efficiency coefficient to match the modeled runoff to observed (Figure 4-1, a-c). The calibrated parameters were Fg=0.87, VIC b-shape parameter=0.3, and T=18 hours. Daily NS is 0.75 and hourly NS is 0.54. The mean annual simulated streamflow minus observed was 4.49 mm. Our model calibration assumes groundwater storage bypasses the Newaukum Urban outlet and joins the channel network farther downstream in the basin. This can be attributed to the location of the small zero-order catchment at the headwaters of a larger watershed (Konrad et al., 2005). We used the model to simulate the catchment hydrologic response for 12 years of hourly observed precipitation data.

The vegetation cover is assumed to be grassed lawns, therefore the effective rooting depth Z_r is set to 0.5 m, the same value used in Wang et al. (2008) and Istanbulluoglu et al. (2012) for grasslands in central Nebraska. The rainfall-runoff depth analysis (Boyd et al. 1993) estimates the EIA to be 20% of the basin, initial abstract is set to 0.16 mm/hr, or 4 mm/day, and leakage is 0.25. The TIA is set to 70% of the basin. The mean annual water balance components and BFI of the observed data, calibrated model, and the 12-year urban and forested simulations are listed in Table 4-1.

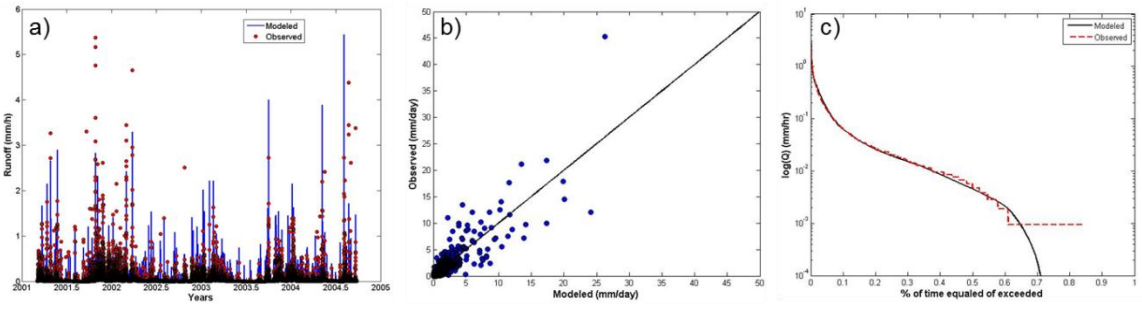

Figure 4-1**. (a) Observed and calibrated model runoff, (b) modeled and observed one-to-one plot, (c) model and observed flow duration curves.**

Table 4-1. **BFI and water balance.**

	Obs 3-year	Urban (3 yr calibration)	Urban (12 yrs)	Forested
BFI	0.4907	0.4324	0.4382	0.8232
Q/P	0.2319	0.2356	0.2315	0.0668
ETa/P		0.3012	0.294	0.5354
Drainage*Fg/P		0.4895	0.4733	0.3971

while the NS coefficient is rather low (but acceptable) the daily value is improved. The flow duration curves show that the model can capture the flow variability in the catchment. Table 4-1 shows good correspondence between observed and model water balance components. For comparison with other studies and the regional hydrology, the forested simulation results are also given in the table. Most notably the ETa/P ratio model is consistent with regional basins. For example, the forested catchment in the Burges et al. (1998) study resulted in an ETa/P ratio (1-R/P) of approximately 0.76.

4.2. Model Simulations

This study models three catchment conditions: urban no treatment (current conditions), forested, and urban with bioretention treatment. To evaluate the bioretention treatment scenario effectiveness in restoring stream health, we calculate the HPR and HPC values of model streamflow output. The indicator results for the 3 years of observed data, urban 3-year model calibration, 12-year urban no treatment simulation, and 12 year forested simulation are shown in Table 4-2. The observed and urban no treatment simulations resulted in ‘very poor’ watershed health and are consistent with each other, suggesting that the model can predict HPR and HPC indices reasonably well. The indicator values of the forested simulation did not fall within the range of Puget Sound data analyzed in the DeGasperi et al. (2009) study and Horner (2012) report. This can be attributed to the fact that the basin recharges a very significant fraction of the infiltrated water to regional groundwater. Fully-forested, predevelopment conditions were simulated

by changing the rooting depth to 1 m, removing all impervious surface coverage, and setting the crop coefficient, K_c, to 1 for conifer trees (Allen et al., 1998). The bioretention treatment included numerous scenarios that vary the size of the bioretention cells and treatment area as shown in Table 4-3.

A single bioretention cell modeled is designed to receive runoff from 1,000 ft^2 of impervious area. The soil is comprised of loamy sand with a porosity of 0.42. The cell was modeled with 2 feet of soil depth following the recommended minimum of 18 inches in the Low Impact Development Technical Guidance Manual for the Puget Sound (PSP and WSU, 2012). The ponding depth is 1 foot following the standard used by the King County of Washington (King County, 2009). While our model simulated grassland dynamics at the pervious layer surface of the bioretention cell, we did not explore the vegetative dynamics for bioretention specific vegetation.

Table 4-2**. HPC and HPR values.**

	Obs 3-year	Urban (3 yr calibration)	Urban (12 yrs)	Forested
HPC	22.67	27.33	27.50	1.17
HPR	285.67	332.67	340.50	21.17

Table 4-3. **Bioretention treatment scenarios.**

	20% Treatment		40% Treatment		60% Treatment	
Bio Cell Footprint (ft)	**Basin Fraction**	**Storage (ft^3)**	**Basin Fraction**	**Storage (ft^3)**	**Basin Fraction**	**Storage (ft^3)**
5x5	0.005	107,134	0.010	214,268	0.015	321,402
10x5	0.010	214,268	0.020	428,536	0.030	642,804
10x10	0.020	428,536	0.040	857,072	0.060	1,285,608
15x10	0.030	642,804	0.060	1,285,608	0.090	1,928,412
15x15	0.045	964,206	0.090	1,928,412	0.135	2,892,618
20x15	0.060	1,285,608	0.120	2,571,216	0.180	3,856,824
20x20	0.080	1,714,144	0.160	3,428,288	0.240	5,142,432
# of cells	**2,329**		**4,658**		**6,987**	

4.3. Sensitivity analysis

This study explored the model's sensitivity to 1) basin fraction treated (from the impervious areas of the catchment) by bioretention cells, 2) a wetter and drier climate than what was observed in the catchment, and 3) total impervious area fraction in the basin to evaluate the sensitivity of catchment characteristics in reducing hydrologic indicators and improving stream health.

In the sensitivity analysis to basin fraction treated, we started by treating the EIA, which was identified to be 20% of the basin. Because a goal of LID is to reduce the amount of EIA, initial analysis distributed bioretention cells to intercept runoff from the EIA fraction before it enters the storm drain. The model was also run for bioretention treatment distributed across 40% and 60% of the basin to evaluate any potential for stream health improvement with increased treatment area beyond EIA. Without bioretention treatment, runoff from the impervious area that is greater than 20% of the catchment would flow onto adjacent pervious surfaces. Intercepting this runoff with bioretention cells will allow for increased infiltration and storage of the stormwater runoff, but any runoff overflowing the ponding layer is routed to the storm drain.

The sensitivity of bioretention cell performance to storm depth was evaluated by simulating a drier and wetter climate. The drier climate was simulated by reducing the observed hourly precipitation depth by 50%, and the wetter climate was simulated by increasing the precipitation depth by 50%. The indicator values for the three climate scenarios with no bioretention treatment are reported in Table 4-4. In all climates, the indicators resulted in 'very poor' stream health for urban no treatment conditions, although there was some variation in the values. The drier climate resulted in an increased number of high pulses while the wetter climate decreased the number of high pulses.

The sensitivity to total impervious fraction of a basin was measured by simulating the basin with reduced impervious coverage. We initially reduced the current condition impervious coverage by half, simulating the impervious area to cover 35% of the basin.

Impervious coverage was reduced further to 20% of the basin, corresponding to the EIA of the current conditions. In each simulation, the fraction of the basin treated was kept constant at 20%.

Table 4.4**. HPC and HPR values for urban no treatment catchment conditions.**

Urban 12 year simulation	HPC	HPR
Current Climate	27.50	340.50
Dry Climate (0.5*P)	29.83	341.17
Wet Climate (1.5*P)	24.92	323.67

Hydrologic indicators were calculated from the model simulated outflow of each treatment scenario. This study compared two different methods for calculating the indicators of the bioretention scenarios. The first method was considered a 'standalone method' with a moving threshold associated with each treatment scenario model run. The threshold was two times the long-term mean of the specific scenario output of interest. The second method identified a single threshold of a base case to identify high pulses in the bioretention scenarios. This threshold was two times the long term mean of the urban no treatment condition. The results of the two methods are presented below.

4.3.1. Current climate treatment simulations (method 1)

The standalone method (method 1) results do not need a base case to identify a threshold and can be used to compare stormwater treatment scenarios across basins. There was some initial improvement in indicator values as bioretention cell size increased, but the scenarios did not improve stream health from the current conditions of 'very poor' (Figure 4-2). As the discharge peaks are reduced with increase treatment, the threshold of each treatment scenario also decreases. Although there is improvement in peak reduction with increase treatment, the improvement is not reflected in the indicator values. The lower threshold still recognizes reduced peaks as high pulses.

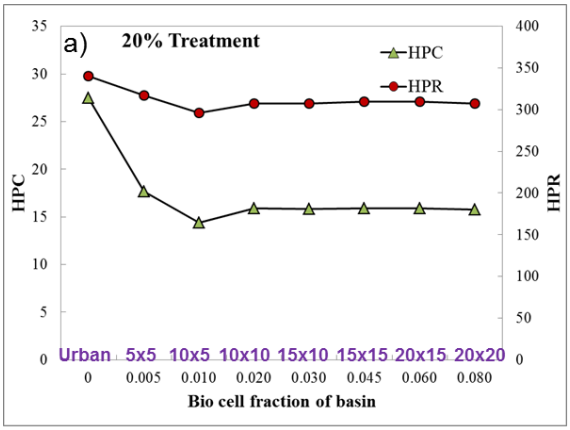

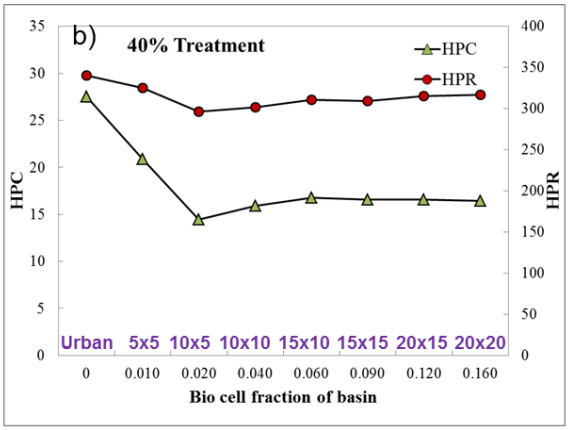

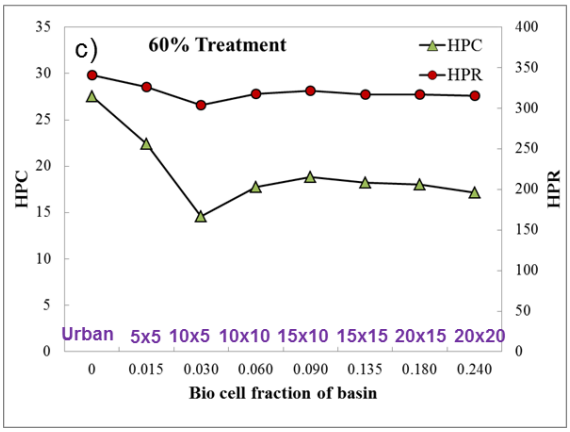

d)

HPC			
Treated Area	20%	40%	60%
5x5	17.67	20.92	22.42
10x5	14.42	14.42	14.58
10x10	15.92	15.92	17.75
15x10	15.83	16.75	18.83
15x15	15.92	16.58	18.25
20x15	15.92	16.58	18.00
20x20	15.75	16.42	17.17

HPR			
Treated Area	20%	40%	60%
5x5	317.42	325.42	326.33
10x5	296.25	296.17	303.75
10x10	307.08	301.75	317.75
15x10	307.00	310.67	321.42
15x15	309.50	309.25	317.08
20x15	309.50	315.50	317.08
20x20	307.00	317.08	315.42

Good/Fair
Fair
Fair/Poor
Poor
Poor/VeryPoor
Very Poor

Figure 4-2**. HPC and HPR results using the the stand-alone method for bioretention treatment scenarios in current catchment condition. a) 20% basin treated, b) 40% basin treated, c) 60% basin treated, d) indicator values.**

4.3.2. Current climate treatment simulations (method 2)

Method 2 uses the same urban no treatment threshold (a base-case threshold) to identify high peaks in the various treatment scenarios. This method is preferred in the rest of the thesis because it provides a comparison relative to the current urbanized case. It is important for us to detect any improvement with respect to the untreated "base" conditions. This method results in the reduction of indicator values corresponding to improve stream health and allows for the identification of the best bioretention scenario to improve watershed health amongst those modeled.

For each basin fraction treatment scenario, there was an initial reduction in indicator values as bioretention cell size increased. As cell size continued to increase, the

treatment scenarios reach a ‘threshold of effectiveness' where increasing the cell size did not result in a significant reduction in indicator value or improvement in stream health. The maximum stream health improvement with the least resources for HPC reduction was ‘poor’ with 10x5 ft cells treating 20% of the basin, ‘fair/poor’ with 10x10 ft cells treating 40% of the basin, and ‘fair’ with 10x10 ft cells treating 60% of the basin. Although there was reduction in HPR values, the reduction was not significant enough to improve stream health from current conditions of ‘very poor’ (Figure 4-3).

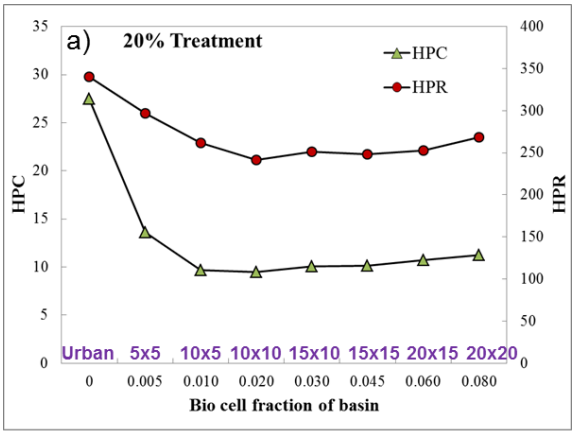

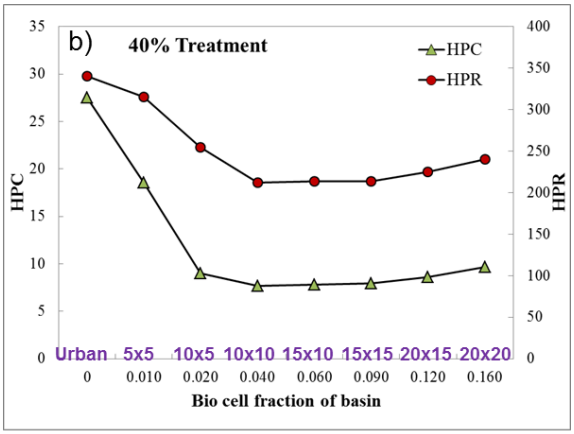

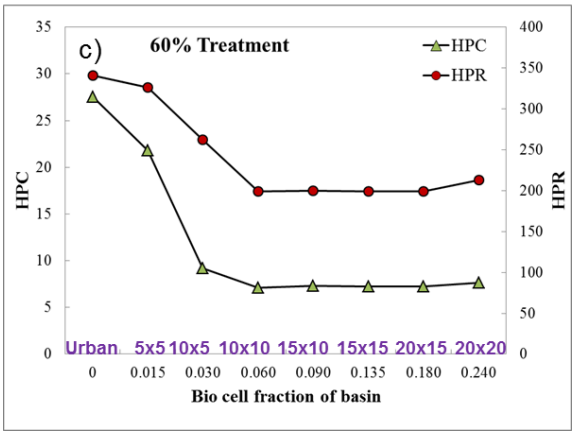

d)

HPC			
Treated Area	20%	40%	60%
5x5	13.58	18.58	21.83
10x5	9.67	9.00	9.17
10x10	9.50	7.67	7.08
15x10	10.08	7.83	7.33
15x15	10.17	7.92	7.25
20x15	10.75	8.58	7.25
20x20	11.25	9.67	7.67

HPR			
Treated Area	20%	40%	60%
5x5	296.67	315.17	326.33
10x5	261.67	254.75	262.08
10x10	241.33	212.00	199.08
15x10	251.58	213.33	199.50
15x15	248.50	213.42	199.42
20x15	253.00	225.17	199.33
20x20	268.17	240.167	213.250

Good/Fair
Fair
Fair/Poor
Poor
Poor/VeryPoor
Very Poor

Figure 4-3**. HPC and HPR results using method 2 for bioretention scenarios in current catchment condition. a) 20% basin treated, b) 40% basin treated, c) 60% basin treated, d) indicator values.**

Figure 4-4 compares the hydrograph of three different treatment scenarios with forested and urban no treatment conditions. The treatment scenarios include a) 5x5 ft cells for 20% treatment or the minimum treatment scenario, b) 10x10 ft cells for 40% treatment, the most effective for 40% treatment, and c) 20x20 ft cells for 60% treatment,

the maximum treatment scenario. In all treatment scenarios, the flashiness of the stream was reduced compared to urban conditions. No level of treatment was able to reduce peaks enough to return the hydrology to forested conditions. While reducing the peak of some of the larger storms, the 10x10 ft cells for 40% treatment increased the discharge of the largest peak for the plotted time period. This is caused by the bioretention antecedent conditions and a large storm occurring causing ponding runoff which is connected to the storm drain, resulting in a larger peak at the outlet of the basin.

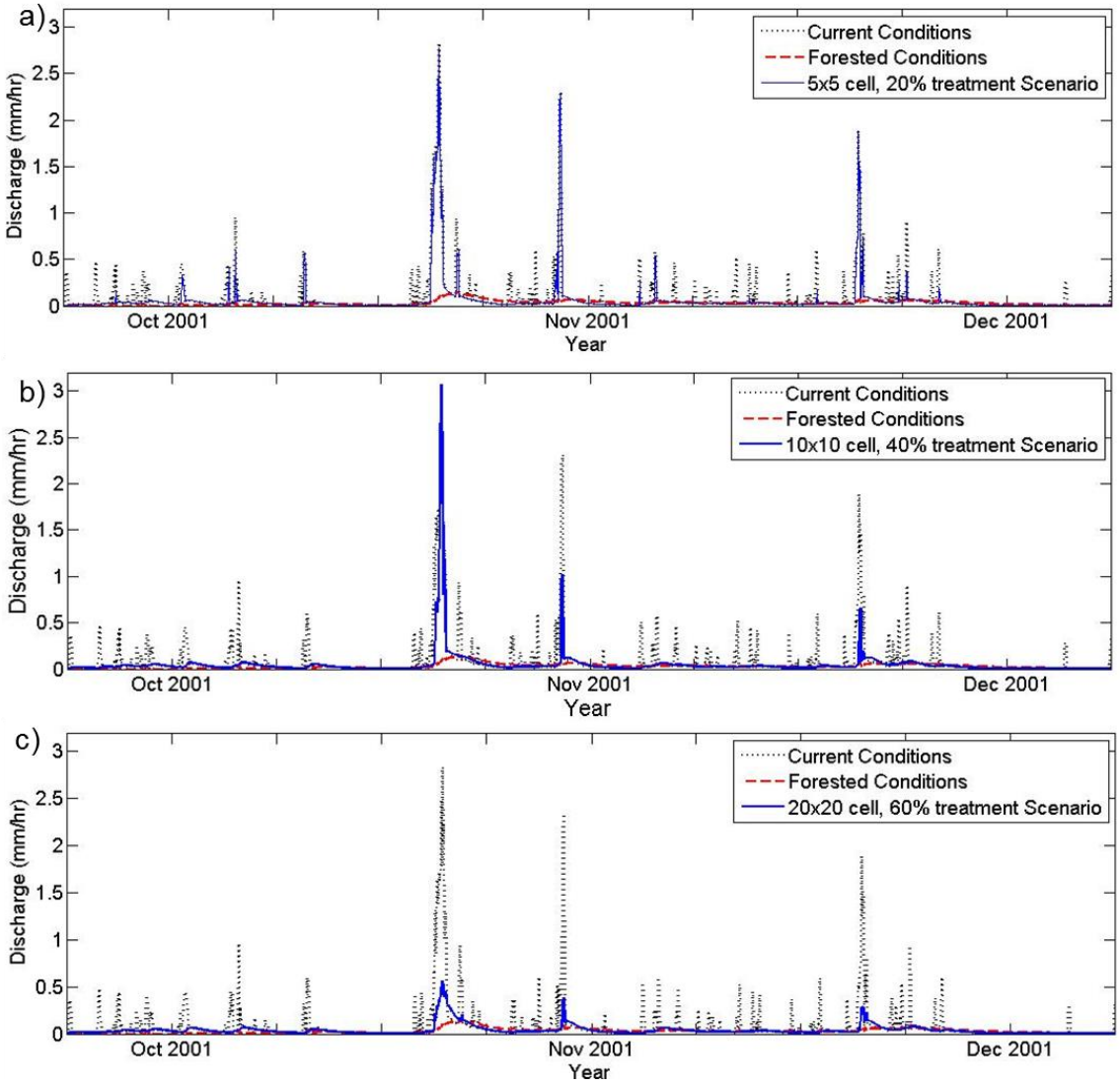

Figure 4-4**. Hydrographs comparing treatment scenarios with forested and urban no treatment conditions. Treatment scenarios are a) the minimum treatment scenario,**

b) the most effective with lowest treatment scenario for 40% treatment, and c) the maximum treatment scenario.

Figure 4-5 plots the depth averaged input into the bioretention cell, the overflow from the ponding layer, and the drainage from the soil layer in a bioretention cell. The figure is plotted for a) 10x5 ft cell, b) 10x10 ft cell, c) 15x15 ft cell, and d) 20x20 ft cell. The input into the bioretention cell includes the precipitation falling on the bioretention cell and the runoff from 1,000 ft^2 of impervious surfaces. Evaluating the bioretention cell at a point reveals the decrease in inflow per unit area as the bioretention cell increases in size, as well as the increase in drainage with respect to the input, and a decrease in the overflow of the ponding layer. Figures 4-4 and 4-5 illustrate increasing the size of the bioretention cells continues to reduce peak discharges from the catchment even though the hydrologic indicators do not significantly decrease. This reflects the limitations of the selected hydrologic indicators for revealing improvements to stream health. Despite this limitation, we use method 2 for the remainder of the study since it initially reflects the improvement of bioretention treatment relative to the base-case, current urban conditions.

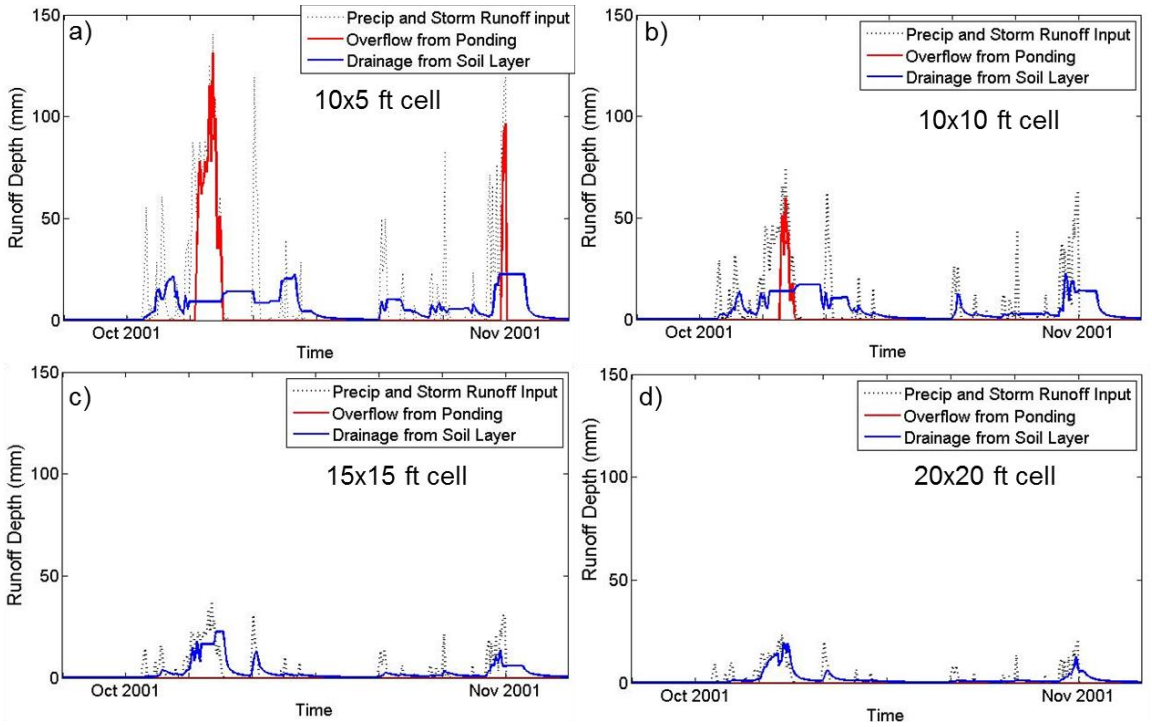

Figure 4-5**. Depth average bioretention input, ponding overflow, and soil drainage at a point for a) 10x5 ft cell, b) 10x10 ft cell, c) 15x15 ft cell, and d) 20x20 ft cell.**

4.3.3. Change in storm depth

A sensitivity analysis of storm depth was performed to determine if bioretention cells were more effective in dry or wet climates. In drier climates, the bioretention scenarios reduced HPC values to 'good/fair' stream health. The 10x10 ft cells were the smallest cell size achieving this level of improvement for each basin fraction treated. The scenarios also reduced HPR values to 'poor/very poor' stream health in the 40% and 60% basin fraction treated (Figure 4-6).

In wetter climates, the bioretention scenarios reduced the HPC values to 'poor' stream health with 40% treatment and to 'fair/poor' stream health with 60% treatment. The scenarios did not reduce HPC with 20% treatment or HPR with any fraction of basin treated enough to improve stream health (Figure 4-7). Overall, bioretention cells were more effective in reducing indicator values in drier climates than wetter climates.

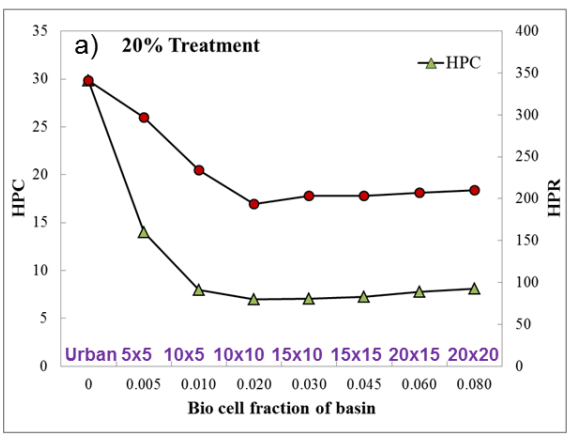

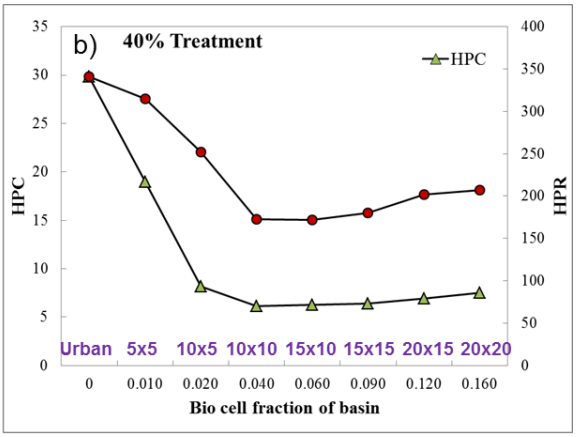

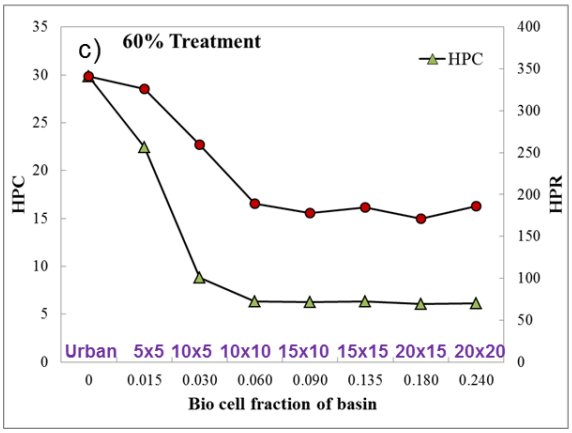

d)

	HPC		
Treated Area	20%	40%	60%
5x5	14.00	19.00	22.42
10x5	8.00	8.17	8.83
10x10	7.00	6.17	6.33
15x10	7.08	6.25	6.25
15x15	7.25	6.42	6.33
20x15	7.75	6.92	6.08
20x20	8.08	7.50	6.17

	HPR		
Treated Area	20%	40%	60%
5x5	296.58	315.00	326.33
10x5	234.17	252.00	259.42
10x10	194.00	172.42	189.25
15x10	203.67	171.83	177.58
15x15	203.58	179.92	185.00
20x15	207.17	202.17	170.83
20x20	210.42	207.25	186.00

Good/Fair
Fair
Fair/Poor
Poor
Poor/VeryPoor
Very Poor

Figure 4-6**. HPC and HPR results for bioretention scenarios in drier climates. a) 20% basin treated, b) 40% basin treated, c) 60% basin treated, d) indicator values.**

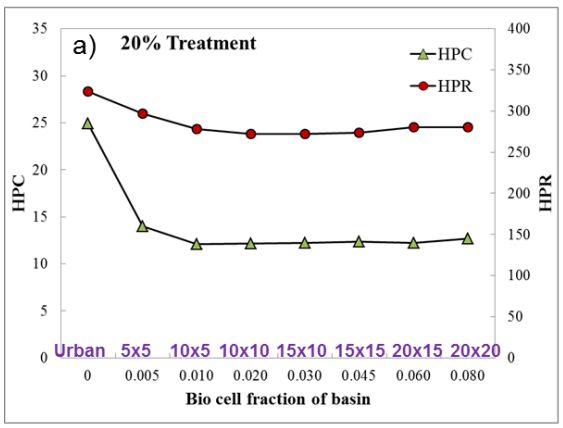

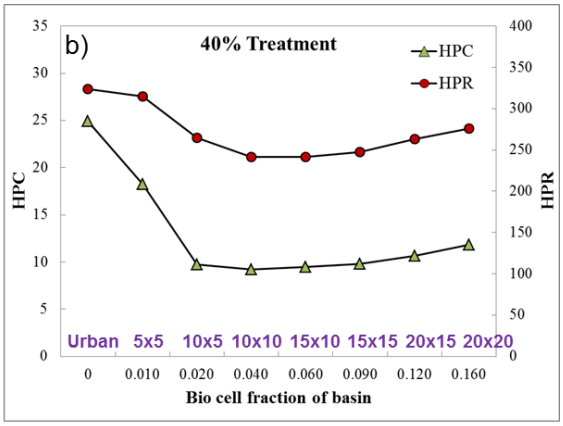

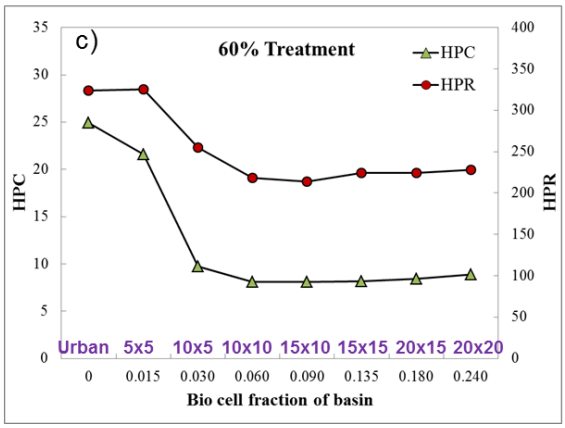

d)

HPC			
Treated Area	20%	40%	60%
5x5	14.00	18.25	21.58
10x5	12.08	9.75	9.75
10x10	12.17	9.25	8.08
15x10	12.25	9.50	8.08
15x15	12.33	9.83	8.17
20x15	12.25	10.67	8.42
20x20	12.67	11.83	8.92

HPR			
Treated Area	20%	40%	60%
5x5	296.83	315.17	325.58
10x5	278.25	265.00	254.75
10x10	272.33	241.42	218.33
15x10	272.33	241.33	214.17
15x15	273.33	247.17	224.50
20x15	280.42	263.58	224.50
20x20	280.42	276.250	228.083

Good/Fair
Fair
Fair/Poor
Poor
Poor/VeryPoor
Very Poor

Figure 4-7**. HPC and HPR results for bioretention scenarios in wetter climates. a) 20% basin treated, b) 40% basin treated, c) 60% basin treated, d) indicator values.**

The flow duration curves for current climate, drier climate, wetter climate, and their respective treatment scenarios are plotted in Figure 4-8. The curves reveal that the bioretention scenarios decreased the peak and high flows, and increase the low and baseflows. We would expect the forested condition (green) to have more baseflow than the urban conditions. Although the values are small, the quick drop off of the low flows for forested conditions may be a result of our model calibration. A large fraction of the drainage is being lost to groundwater and bypassing the Newaukum Urban outlet. Further examination of the basin groundwater storage is needed for forested simulations.

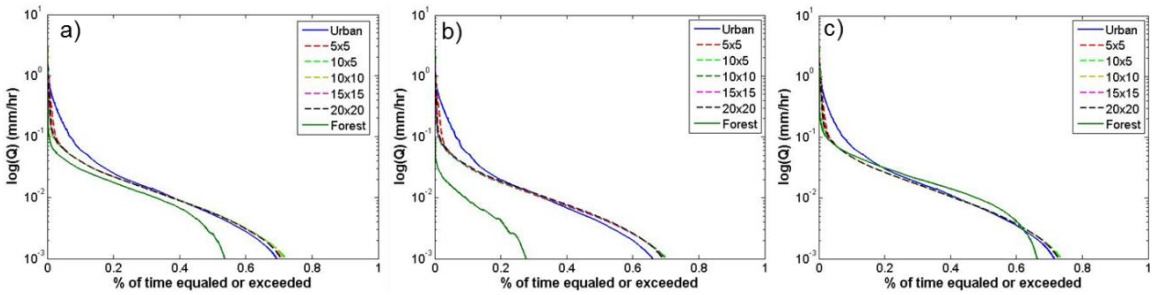

Figure 4-8**. Flow duration curves for a) current climate condition treatment scenarios, b) drier climate treatment scenarios, and c) wetter climate treatment scenarios.**

4.3.4. Reducing Impervious fraction

The total impervious fraction of the basin is 70%. We reduced the total impervious area of the basin the 35% (half of the current fraction, Figure 4-9) and 20% (same size as EIA, Figure 4-10) of the basin to evaluate the impact on indicator reduction and stream health improvement. In each imprevious fraction reduction, the bioretention cells treated 20% of the catchment. Therefore, when the basin fraction was reduced to 35%, 20% of the basin was treated EIA and 15% was DIA. When the impervious fraction is reduced to 20%, all of the impervious area is treated with no stormwater runoff flowing into the pervious areas. Reducing the impervious fraction of the basin increased the reduction in hydrologic indicators and resulted in a greater improvement of watershed health. Both impervious fraction reduction scenarios resulted in a similar response of improving stream health to ‘good/fair’ for HPC and ‘fair/poor’ for HPR.

Figure 4-11 plots the flow duration curves for the various impervious fractions. The difference between the medium flows of urban and forested decreased as the impervious fraction was reduced in the catchment. The bioretention scenarios were more effective increasing baseflow from urban conditions as impervious fraction decreased.

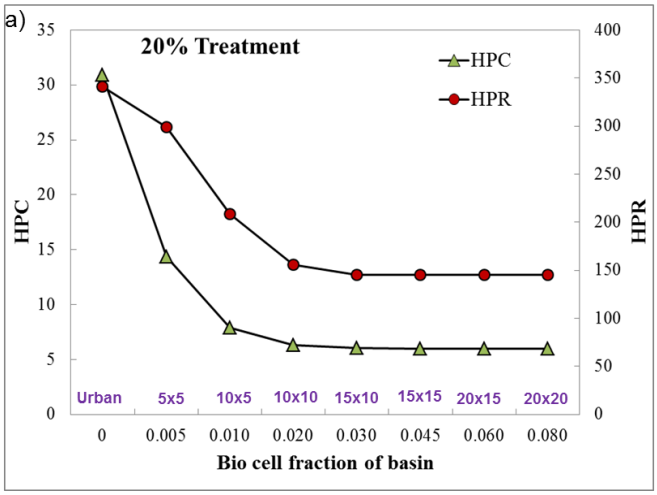

b)	HPC
Treated Area	20%
5x5	14.33
10x5	7.92
10x10	6.33
15x10	6.08
15x15	6.00
20x15	6.00
20x20	6.00

	HPR
Treated Area	20%
5x5	298.75
10x5	208.33
10x10	155.83
15x10	145.00
15x15	145.00
20x15	145.00
20x20	145.00

	HPC	HPR
Urban	30.92	341.00

Good/Fair
Fair
Fair/Poor
Poor
Poor/VeryPoor
Very Poor

Figure 4-9. **Indicator values for catchment with 35% total impervious fraction, and 20% of basin treated with bioretention cells.**

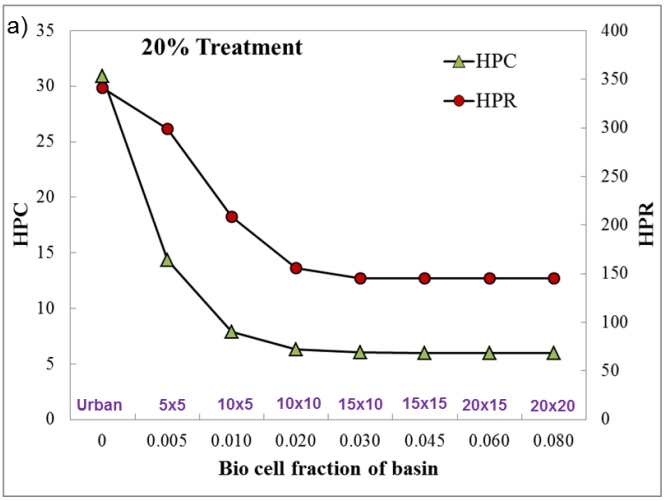

b)	HPR
Treated Area	20%
5x5	298.75
10x5	208.33
10x10	155.83
15x10	145.00
15x15	145.00
20x15	145.00
20x20	145.00

	HPC
Treated Area	20%
5x5	14.33
10x5	7.92
10x10	6.33
15x10	6.08
15x15	6.00
20x15	6.00
20x20	6.00

	HPC	HPR
Urban	30.92	341.00

Good/Fair
Fair
Fair/Poor
Poor
Poor/VeryPoor
Very Poor

Figure 4-10. **Indicator values for catchment with 20% total impervious fraction, and 20% of basin treated with bioretention cells.**

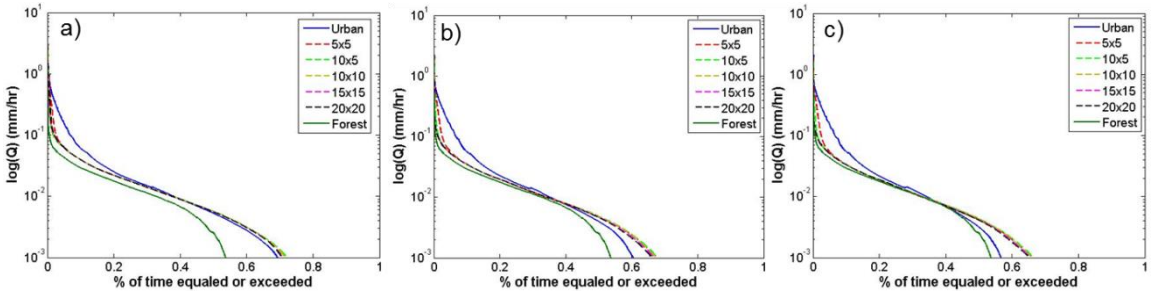

Figure 4-11**. Flow duration curves for a) 70% total impervious fraction (current catchment) treatment scenarios, b) 35% total impervious fraction and 20% of basin treated, and c) 20% total impervious fraction and 20% of basin treated.**

5. CONCLUSIONS

Land development continues to replace forested areas in the Puget Sound lowlands. This urbanization alters the hydrologic response of the landscape resulting in greater storm runoff volumes and increased streamflow peaks that erode stream channels and impair biological health. In the last decade, stormwater management shifted from a structural approach emphasizing the efficient conveyance of stormwater runoff away from urban areas to one focusing LIDs and controlling stormwater runoff at the source.

Current stormwater management in the Puget Sound region requires the control of runoff from new development or redevelopment of a site (King County, 2012). This study takes a watershed approach to stormwater management and develops the lumped UEM model to simulate urbanized catchment hydrology and evaluate the effectiveness of bioretention facilities for improving stream health. Bioretention performance is measured by comparing the reduction of hydrologic indicators, HPC and HPR, correlated with biological health. A sensitivity analysis explored the catchment response to basin fraction treated, storm depth, and impervious surface coverage.

Interestingly, in all simulations increasing the size of bioretention cells for the same treatment area reached a ‘threshold of effectiveness’ for stream health improvement. Furthermore, the HPC and HPR curves decline and reach a threshold in parallel. Although there was an initial improvement in stream health with increasing bioretention cell size, as cell size continued to increase there was no reduction of indicator values associated with any further improvements in stream health. Controlling stormwater at the source reduced the number of high pulses in a water year to improve stream health but was less effective in reducing the period of time the pulses occurred.

The results also illustrate the limitations of HPC and HPR for identifying hydrologic improvement from bioretention treatment in the catchment. The treated basin hydrographs reveal a greater reduction in storm event peaks with increased treatment even though the calculated indicators show no improvement in stream health. The hydrologic indicators are not sensitive enough to reflect these reductions unless they fall below the threshold for identifying high pulses.

The indicators were not effective at showing bioretention treatment hydrologic improvements when calculated using a scenario specific threshold for identifying high pulses. This stand-alone method would allow comparison of the degree of catchment treatment across basins. The method that was more effective for relative comparison of bioretention treatment scenarios required a base-case catchment condition to calculate a single threshold to compare all treated basin hydrologic response.

The greatest improvement in hydrologic indicators associated with restoring stream health were bioretention treatment in drier climates or basins with reduced total impervious fraction. Although there is still a 'threshold of effectiveness' for bioretention scenarios, bioretention treatment was able to reduce the number of high pulses associated with 'good' stream health. These results emphasize the impact climate and degree of catchment urbanization will have on bioretention performance in reaching hydrologic goals or targets.

In the analysis of bioretention treatment performance, we discovered limitations when using HPC and HPR indicators to reveal hydrologic improvement. This study found that indicator values were not sensitive enough to reflect all peak reductions occurring with treatment. Although the hydrologic indicators may not represent the entire picture, they did respond to bioretention treatment and can be used to identify some improvement in catchment hydrologic response. If hydrologic indicators are used to establish stream health targets for stormwater management, evaluating the stormwater facility needs at a catchment scale rather than the site scale may reveal the most effective solution for a region with the least investment or resources.

6. REFERENCES

Allen, R. G., L.S. Pereira, D. Raes and M. Smith (1998). Crop evapotranspiration, guidelines for computing crop water requirements, *FAO Irrigation and Drainaige. Paper 56, Food and Agriculture Organisation of the United Nations*, Rome, Italy. 300 pp.

ASCE-EWRI (2005). The ASCE Standardized Reference Evapotranspiration Equation. Report of the Task Committee on Standardization of Reference Evapotranspiration. Environmental and Water Resources Institute of the American Society of Civil Engineers, Reston, Virginia, USA.

DeGasperi, C. L., H. B. Berge, K.R. Whiting, J. J. Burkey, J. L. Cassin, and R. R. Fuerstenberg (2009). Linking hydrologic alteration to biological impairment in urbanization streams of the Puget Lowland, Washington, USA. *Journal of American Water Resource Association,* 45(2), 512-533.

Booth, D.B., J.R. Karr, S. Schauman, C.P. Konrad, S.A. Morley, M.G. Larson, and S.J. Burges (2004). Reviving Urban Streams: Land Use, Hydrology, Biology, and Human Behavior. *Journal of the American Water Resources Association*, 40,1351-1364.

Boyd, M.J., M. C. Bufill, and R. M. Knee (1993). Pervious and impervious runoff in urban catchments, *Hydrological Sciences*, 38(6), 463-478.

Boyd, M.J., M. C. Bufill, and R. M. Knee (1994). Predicting pervious and impervious storm runoff from urban drainage basins, *Hydrological Sciences*, 39(4), 321-332.

Burges, S. J., M. S. Wigmosta, and J. M. Meena (1998). Hydrological effects of land-Use change in a zero-order catchment. *Journal of Hydrologic Engineering*, 3, 86-97.

Campbell, G. S. (1974). A simple method for determining unsaturated conductivity from moisture retention data, *Soil Sciences*, 117, 3311-314.

Chapman, T. (1991). Comment on ‘‘Evaluation of automated techniques for base flow and recession analyses’’ by R. J. Nathan and T. A. McMahon, *Water Resources Research*, 27, 1783– 1784.

Coffman, Larry S. (2000). Low Impact Development Design: A New Paradigm for Stormwater Management Mimicking and Restoring the Natural Hydrologic Regime. Conference Proceedings from the National Conference on Tools for Urban Water Resource Management & Protection.

Cuo, L., D. P. Lettenmaier, M. Alberti and J.E. Richey (2009). Effects of a century of land cover and climate change on the hydrology of the Puget Sound basin, *Hydrological Processes*, 23, 907-933.

Davis, A. L. (2005). Green engineering principles promote low impact development, *Environmental Science and Technology*, 39, 338A-344A.

Fore, L.S., J.R. Karr and R.W. Wisseman (1996). Assessing Invertebrate Responses to Human Activities: Evaluating Alternative Approaches. *Journal of the North American Benthological Society* 15(2), 212-231.

Herrera (2007). Water Quality Statistical and Pollutant Loadings Analysis, Green-Duwamish Watershed Water Quality Assessment. Prepared for King County Department of Natural Resources and Parks by Herrera Environmental Consultants, Inc., Seattle, Washington. January 19, 2007.

Hino, M., and M. Hasabe (1984). Identification and prediction of nonlinear hydrologic systems by the filter-separation autoregressive (AR) method: extension to hourly hydrologic data, *Journal of Hydrology*, 68, 181-210.

Horner, R.R., D.B. Booth, A. Azous, and C.W. May (1997). Watershed Determinants of Ecosystem Functioning. In L.A. Roesner (ed.), Effects of Watershed Development and Management on Aquatic Ecosystems, *American Society of Civil Engineers,* New York, NY, 251-274.

Horner, R. (2011). Development of Flow and Water Quality Indicators. Unpublished Status Report.

Horner, R. (2012). Development of Flow and Water Quality Indicators. Unpublished Status Report.

Istanbulluoglu, E., T. Wang, and D. A. Wedin (2012). Evaluation of ecohydrologic model parsimony at local and regional scales in a semiarid grassland ecosystem, *Ecohydrology*, 5, 121-142.

Karr, J.R., and C.O. Yoder (2004). The Biological Assessment and Criteria Improve Total Maximum Daily Load Decision Making, *Journal of Environmental Engineering*, 130 (6), 594-604.

King County (2009). 2009 Surface Water Design Manual. King County, DNRP, Water and Land Resources Division.

King County (2012). 2012 Stormwater Management Program. King County, DNRP, Water and Land Resources Division.

Konrad , C. P., D. B. Booth and S. J. Burges (2005). Effects of urban development in the Puget Lowland, Washington, on interannual streamflow patterns: Consequences for channel form and streambed disturbance, *Water Resources Research*, 41, 1-15.

Konrad , C. P. and S. J. Burges (2001). Hydrologic Mitigation Using On-Site Residential Storm-Water Detention, *Journal of Water Resources Panning and Management*, 127 (2), 99-107.

Laio, F., A. Porporato, L. Ridolfi, I Rodriguez-Iturbe (2001). Plants in water controlled ecosystems: Active role in hydrologic processes and response to water stress II. Probabilistic soil moisture dynamics, *Advances in Water Resources*, 24, 707-723.

Liang, X., Lettenmaier, D. P., Wood, E. F. & Burges, S. J. (1994). A Simple hydrologically Based Model of Land Surface Water and Energy Fluxes for GSMs, Journal of Geophysical Research, 99(D7), 14,415-14,428.

Latterell, J; J. Vanderhoof, J. Burkey, J. Bethel, K. Johnson (2007). Newaukum Creek Basin Characterization Project Report. King County, DNRP, Water and Land Resources Division.

Linsley, R. K., M.A. Kohler, and J.L.H. Paulhus (1958). Hydrology for Engineers, McGraw-Hill, New York.

May, C. R. Horner, J. Karr, B. Mar, and E. Welch. 1997. Effects of Urbanization on Small Streams In the Puget Sound Lowland Ecoregion. *Watershed Protection Techniques*, 2(4), 483-494.

Morley, S. A., and J. R. Karr (2001). Assessing and restoring the health of urban streams in the Puget Sound basin, *Conservation Biology*, 16(6), 1498-1509.

Nathan, R. J., and T. A. McMahon (1990). Evaluation of automated techniques for base flow and recession analyses, *Water Resources Research*, 26, 1465– 1473.

PGCo(Prince George's County, Maryland) (1999). Low-Impact Development Design Strategies: An Integrated Design Approach. Prince George's County, Maryland. Department of Environmental Resources, Programs and Planning Division.

PGCo(Prince George's County, Maryland) (1999b). Low-Impact Development Hydrologic Analysis. Prince George's County, Maryland. Department of Environmental Resources, Programs and Planning Division.

PGCo (Prince George's County, Maryland) (2007). Bioretention manual. Prince George's County, Maryland. Department of Environmental Resources, Programs and Planning Division.

Puget Sound Partnership and the Washington State University Extension (PSP and WSU) (2012). Low Impact Development Technical Guidance Manual for Puget Sound.

Smakhtin, V. U. (2001). Low flow hydrology: A review, *Journal of Hydrology.*, 240, 147– 186.

Shoemaker, L., J. Riverson Jr., K. Alvi, J. X. Zhen, S. Paul, and T. Rafi (2009). SUSTAIN - A Framework for Placement of Best Management Practices in Urban Watersheds to Protect Water Quality. EPA/600/R-09/095. U.S. Environmental Protection Agency, Water Supply and Water Resources Division, National Risk Management Research Laboratory, Cincinnati, OH.

Sujono, J., S. Shikasho, and K. Hiramatsu (2004). A comparison of techniques for hydrograph recession analysis, *Hydrological Processes*, 18, 403-313.

USEPA (U. S. Environmental Protection Agency) (2000). Low Impact Development (LID): A Literature Review. Office of Water, Washington, DC.

Wang, T., E. Istanbulluoglu, J. Lenters, and D. Scott (2009). On the role of groundwater and soil texture in the regional water balance: An investigation of the Nebraska Sand Hills, USA, *Water Resources Res*earch, 45, W10413, doi:10.1029/2009WR007733.